
A MULTIFRACTAL APPROACH TO THE STRENGTH AND TOUGHNESS SCALING OF CONCRETE STRUCTURES

A. Carpinteri and B. Chiaia,
Department of Structural Engineering, Politecnico di Torino
10129 Torino, Italy

Abstract

The phenomenon of the size-dependence of concrete tensile strength and fracture energy is discussed. The scaling of the nominal quantities can be consistently interpreted by means of a multifractal model, the influence of microstructural disorder being predominant at the smallest scales. At the larger scales, the fields homogeneization comes into play, allowing for the mean-field definition of asymptotic properties. Two Multifractal Scaling Laws (MFSL) are proposed, respectively for tensile strength and fracture energy. By means of best-fitting of the experimental data, the full range of the scaling is described and the asymptotic values of σ_u and \mathcal{G}_F , valid for real-sized structures, can be determined.

1 Theoretical and experimental evidence of multifractality in the phenomenon of fracture

Criticality is very evident in the phenomenon of fracture of disordered materials: at the critical point a transition occurs in the evolutive behavior of microcracks. Whilst, before the critical strain ε_u , virtually no microcrack can propagate to the structural scale, thus resulting in the macroscopic integrity of the body, beyond ε_u the correlation length of the

phenomenon increases tending to infinite and microcracks suddenly coalesce, yielding the catastrophic fracture of the body.

On the basis of this evidence, the mechanical quantities involved in the phenomenon, respectively the fracture energy \mathcal{G}_F and the tensile strength σ_u , can be treated as critical parameters. Hence, in the asymptotic limit of the critical point, they behave as *self-similar functions* of the independent variables. As it has been widely demonstrated, self-similarity appears to be the fundamental character of critical phenomena, either from the Physics or from the Topology point of view (Wilson, 1971). At the critical point, the system shows similar fluctuations at all length scales or, which is the same, no characteristic internal length is present and the correlation length tends to infinite. From the geometrical point of view, this means that the system looks statistically the same at all length scales, that is, is a *fractal*.

Topological self-similarity (fractality) has been detected in the microstructures of many heterogeneous materials: the networks of surface cracks (Herrmann & Roux, 1990), the fracture surfaces of concrete (Carpinteri & Chiaia, 1995a), rocks and metals (Mandelbrot et al., 1984) and the distributions of microcracks in the bulk of a stressed body (Barenblatt & Botvina, 1983) were shown to share fractal properties in a well defined scale range. An adequate modelization of the microstructure is therefore necessary in order to avoid the limitations of a classical *mean-field* approach, where disorder is simply averaged in an elementary representative volume. On the contrary, the fracture of brittle materials has to be considered as a *cooperative phenomenon* with interactions at all length scales: only in this way the scaling behavior of the mechanical quantities can be consistently explained.

Multi-scale phenomena, such as phase transitions, percolations and diffusion-limited aggregations, are nowadays successfully interpreted by means of fractal models. The non-integer topological dimensions of the domains on which the physical quantities are defined assume a deep significance with respect to the scaling behavior of the same quantities (Carpinteri, 1994a). A fundamental distinction among these topologies has to be pointed out: the so-called “*invasive*” fractals, that is, the spatial domains whose topological dimension Δ is strictly larger ($\Delta = 2 + d_G$) than their projection's euclidean dimension, usually produce *positive* scaling of the quantities (\mathcal{G}_F) defined over them. In the case of brittle fracture, the von Koch triadic curve (Fig. 1a) is an example of an invasive fractal set embedded in the bidimensional plane, which is well-suited for the modelization of the energy dissipation space.

On the contrary, “*lacunar*” fractals like the middle-third Cantor set (Fig. 1b) possess topological dimension Δ strictly lower than that of the domain where they are contained ($\Delta = 2 - d_G$), and therefore provide

negative scaling of the quantities (σ_u) defined over them. The rarefied (damaged) ligament of an heterogeneous solid subjected to tensile loading can be consistently modeled by means of this kind of fractal sets.

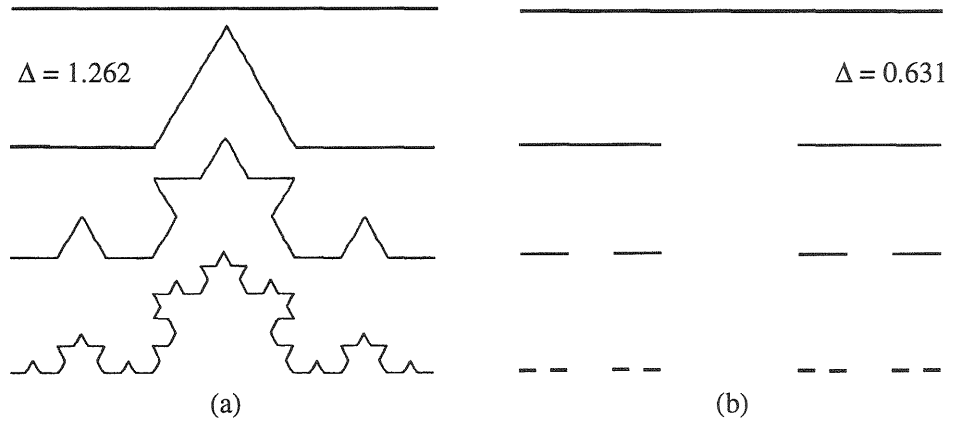


Fig. 1. Invasive (a), and lacunar (b) fractal domains.

An upper and a lower bound are present in the scaling range of natural fractal sets: consequently, a transition from the fractal (disordered) regime at the microscopic level towards an euclidean (homogeneous) regime at the largest scales always occurs. The upper bound is represented by the macroscopic size of the object, whilst the lower one is related to the size of the smallest measurable particles, these being the grains, in the case of metals, the crystals, in the case of rocks, and the aggregates, in the case of concrete. It can be argued that the presence of this *internal length*, typical of each microstructure, inhibits the development of a perfect self-similar scaling through the whole scale range, whereas mathematical fractals like those in Fig. 1, lacking absolutely of any characteristic length, exhibit uniform (monofractal) scaling without any bound.

Experimental investigations were carried out by the authors (Carpinteri et al., 1995a) on concrete fracture surfaces. Application of the *box-counting* method to digitized fracture profiles (Fig. 2a) showed that not a unique value of the fractal dimension can be determined, but a continuously decreasing slope in the bilogarithmic diagram is obtained (Fig. 2b), and an infinity of exponents is thus necessary to describe the entire scaling range (*geometrical multifractality*).

The aforementioned investigations showed also that the highest possible disorder in the microstructures is represented by a *Brownian disorder*, in the sense that a fractional topological increment d_G (or decrement, in the case of d_G) equal to 0.5 seems to be the highest in the limit of the microscopic scales of observation. Such a thermodynamical

assumption is confirmed by the multitude of fractal measurements in different materials that have been reported in the literature. On the other hand, an indirect validation of this assumption comes from the experimental determination of the size-effect exponents, either in the case of fracture energy (Carpinteri & Chiaia, 1995) or in the case of tensile strength (Carpinteri et al., 1995), that have never been measured larger than $\pm 1/2$.

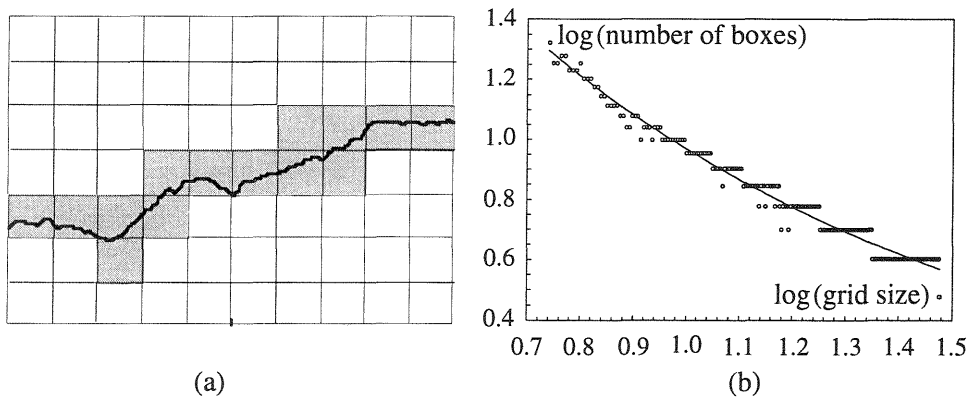


Fig. 2. Experimental detection of multifractality: box-counting method.

2 Dimensional Analysis vs. Renormalization Group

Let us consider a physical quantity q , defined as a function of other n quantities: $q = F(q_1 \dots q_k, q_{k+1} \dots q_n)$, where $(q_1 \dots q_n)$ are the so-called “governing parameters” of the phenomenon. They can be split into parameters $(q_1 \dots q_k)$ with independent physical dimensions and parameters $(q_{k+1} \dots q_n)$ whose dimensions are combinations of the k independent parameters’ ones. The well-known Buckingham’s theorem states that any valid physical relation can be expressed as a function Π of $(n-k)$ non-dimensional quantities $(N_1 \dots N_{n-k})$, which are combinations of the (n) governing parameters:

$$\Pi = \mathbf{G}(N_1, N_2, \dots, N_{n-k}). \quad (1)$$

The concept of *external similarity*, claimed by Dimensional Analysis, states that two or more physical phenomena are *similar* if they differ only in the numerical value of the governing parameters, that is, if the corresponding non-dimensional quantities (the *similarity parameters*) coincide. This concept can be extended from the comparison between two different phenomena to the behavior of a single phenomenon at various scales of observation (*internal similarity* or *self-similarity*). A physical

process is called *self-similar* if the spatial distribution of its properties at a certain scale of observation can be obtained by means of a simple similarity transformation from the distribution of the same properties at another scale. Three situations can be encountered, to which three particular categories of physical phenomena correspond: complete self-similarity, incomplete self-similarity, and absence of self-similarity (Barenblatt, 1993).

An example of complete self-similarity is provided by Linear Elastic Fracture Mechanics: in this context, a typical similarity parameter is represented by the *Brittleness Number* $s = K_{IC}/\sigma_u b^{1/2}$ (Carpinteri, 1986), which allows one to define the *degree of ductility* of a structure, regardless of the specific structural shape and loading condition. All the self-similarity parameters are deduced by the usual procedures of Dimensional Analysis, obtaining, in this way, the so-called “canonical” dimensions. The simple comparison between the physical dimensions of the ultimate tensile stress σ_u ($[F][L]^{-2}$) and of the stress-intensity factor K_{IC} ($[F][L]^{-3/2}$) provides the exponent of the size-scaling law for strength:

$$\sigma_u \sim b^{-1/2}, \quad (2)$$

which implies a constant $-1/2$ slope in the bilogarithmic diagram, as is shown in Fig. 3.

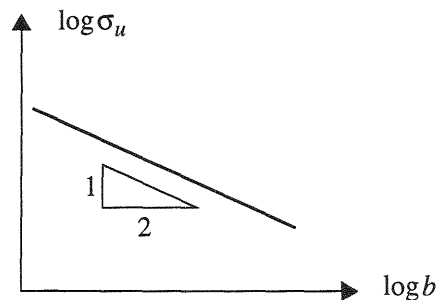


Fig. 3. Size-effect on nominal tensile strength according to LEFM.

In the case of three-point bending of a notched elastic-perfectly plastic beam, where brittle fracture interacts with plastic collapse, Dimensional Analysis yields:

$$\frac{F}{\sigma_y b^2} = \Pi \left[\frac{\mathcal{G}_{IC}}{\sigma_y b}, \frac{a_0}{b}, \frac{l}{b}, \frac{t}{b} \right], \quad (3)$$

where σ_y is the yielding stress, \mathcal{G}_{IC} is the fracture energy, b is the beam

depth (reference size), l and t are the beam span and thickness, respectively, and a_0 is the initial notch depth. The strength and toughness parameters, σ_y e \mathcal{G}_{IC} respectively, are thus defined in a traditional manner, that is, as material constants characterized by the canonical physical dimensions ($[F][L]^{-2}$ and $[F][L]^{-1}$). By inserting the *Energy Brittleness Number* $s_E = \mathcal{G}_{IC} / \sigma_y b$ into Eq. (3), one notes that, in the limit of a_0 tending to zero, function Π converges towards a finite non-zero value:

$$\lim_{\alpha \rightarrow 0} \frac{F}{\sigma_y b^2} = \Pi(s_E; 0, \lambda, \tau) = \frac{\tau}{\lambda}, \tag{4}$$

where the greek letters indicate the corresponding non-dimensional quantities. Eq. (4) represents the classical Limit Analysis solution, obtained as the midspan singularity tends to zero.

If the behavior of Eq. (3) is investigated as the reference size b tends to zero or to infinity, recalling the fundamental Griffith solution ($F/b^2 \sim b^{-1/2}$), it can be shown (Carpinteri, 1995) that the limit becomes:

$$\lim_{b \rightarrow 0} \frac{F}{\sigma_y b^2} = s_E^{1/2} \lim_{b \rightarrow 0} \bar{\Pi} \left(\frac{\alpha}{s_E^{\beta_2}}, \frac{\lambda}{s_E^{\beta_3}}, \frac{\tau}{s_E^{\beta_4}} \right). \tag{5}$$

A set of real numbers ($\beta_2, \beta_3, \beta_4$) can therefore be determined, such that the limit can still be uniquely defined, but now the strength and toughness parameters, σ_y and \mathcal{G}_{IC} , being not anymore scale-invariant material constants, depend on the considered structural size (*size-effect*).

The scale-independence can be pursued only by abandoning the canonical physical dimensions, and moving to the so-called *anomalous* dimensions, which cannot be determined by Dimensional Analysis arguments but only by means of the Renormalization Group procedure (Carpinteri, 1994b). Moreover, the critical exponents ($\beta_2, \beta_3, \beta_4$) generally turn out to be non-integer numbers. This is the case of *incomplete similarity of the phenomenon with respect to the parameter b*.

3 Incomplete self-similarity and monofractal scaling laws

Starting from the hypothesis of incomplete self-similarity (fractal topologies), a simple Renormalization Group can be deduced for the fracture energy \mathcal{G}_F , by considering a cascade of observation scales, ranging from the conventional macroscopic one (see the classical RILEM definition of surface fracture energy (1985)), to the microscopic one where the dissipation space is considered as a monofractal domain with

topological dimension comprised between 2 and 3. With reference to Fig. 1a, the nominal fracture energy \mathcal{G}_F ($[J][L]^{-2}$) at the macroscopic scale is supposed to be dissipated over the nominal area A_0 , whereas, increasing the resolution, more and more details of the “surface” appear, yielding an increased nominal area A_1 and a corresponding fictitious fracture energy \mathcal{G}_1 . At the next step, A_2 and \mathcal{G}_2 can be defined, and so on. In the limit of the microscopic scale, the *measure* A^* of the asymptotic invasive fractal set has to be considered, and therefore the *renormalized fracture energy* \mathcal{G}_F^* comes to assume the anomalous fractional dimensions:

$$\left[\mathcal{G}_F^* \right] = [J][L]^{-(2+d_{\mathcal{G}})}, \quad (6)$$

where $d_{\mathcal{G}}$ is the fractional topological increment of the dissipation space due to disorder ($0 < d_{\mathcal{G}} < 1$). Note that, from Eq. (6), the dissipated energy in the fracture process is considered intermediate between purely surface energy (which is the hypothesis of LEFM) and volume energy (which is the approach of Limit Analysis and Damage Mechanics).

The invariance of the total dissipated energy ΔW with respect to the observation scale has to be maintained. The following group of transformations can be therefore deduced:

$$\Delta W = \mathcal{G}_F A_0 = \mathcal{G}_1 A_1 = \dots = \mathcal{G}_F^* A^*. \quad (7)$$

From the definition of Hausdorff measures, if b is a characteristic reference size of the structure, the following dimensional relations hold: $A_0 \sim b^2$ and $A^* \sim b^{2+d_{\mathcal{G}}}$. By equating the second and the last member in Eq. (7), the scaling of nominal fracture energy is obtained as:

$$\mathcal{G}_F \sim \mathcal{G}_F^* b^{d_{\mathcal{G}}}. \quad (8)$$

The *renormalized fracture energy* \mathcal{G}_F^* represents a true material constant, in the sense that scale-invariance can be satisfied only by abandoning the canonical euclidean dimensions. In the bilogarithmic diagram $\log \mathcal{G}_F$ vs. $\log b$, Eq. (8) implies the linear increase of the nominal fracture energy with increasing structural size, with positive slope equal to $d_{\mathcal{G}}$ (Fig. 4a).

The same arguments can be adopted in the case of tensile strength. With reference to Fig. 1b, a cascade of scales can be considered, taking into account the (incomplete) self-similar weakening of the resisting material ligament due to the defects and microcracks distribution at all the length scales. At the macroscopic scale, the nominal tensile strength σ_u ($[F][L]^{-2}$) is supposed to be carried by the nominal area A_0 , whereas, increasing the

resolution, more and more gaps in the ligament are revealed, yielding a decreased nominal area A_1 and a corresponding fictitious micro-stress σ_1 . At the next step, A_2 and σ_2 can be defined, and so on. In the limit of the microscopic scale, the *measure* A^* of the asymptotic lacunar set has to be considered: hence, the *renormalized tensile strength* σ_u^* is characterized by the following anomalous fractional dimensions:

$$[\sigma_u^*] = [F][L]^{-(2-d_\sigma)}, \quad (9)$$

where d_σ is the fractional topological decrement ($0 < d_\sigma < 1$) of the ligament due to disorder. Since the external force F is a macro-parameter, in the sense that it is invariant with respect to the scale of observation, the following cascade can be written:

$$F = \sigma_u A_0 = \sigma_1 A_1 = \dots = \sigma_u^* A^*. \quad (10)$$

By equating the second and the last member in Eq. (10), and considering the non-integer measure of the set $(2-d_\sigma)$, the scaling of nominal tensile strength is obtained as:

$$\sigma_u \sim \sigma_u^* b^{-d_\sigma}. \quad (11)$$

The *renormalized tensile strength* σ_u^* represents, in this case, the scale-invariant material constant. In the bilogarithmic diagram $\log \sigma_u$ vs. $\log b$, Eq. (11) implies the linear decrease of the nominal tensile strength with increasing structural size, with negative slope equal to $-d_\sigma$ (Fig. 4b).

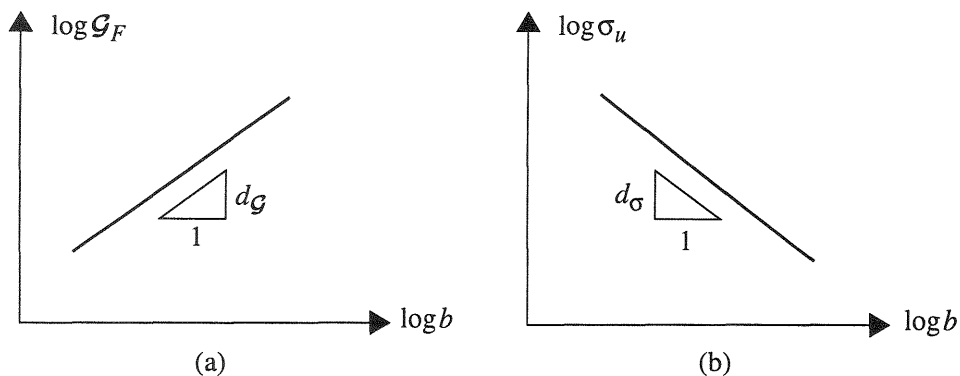


Fig. 4. Monofractal scaling of fracture energy (a) and tensile strength (b).

The non-standard scaling of the critical quantities involved in the phenomenon of brittle fracture has been obtained, in the hypothesis of incomplete self-similarity, by means of Renormalization Groups. On the

other hand, for structural size tending to infinite, an absurd infinite value of \mathcal{G}_F would be predicted by the monofractal scaling of Eq. (8), as well as an unreal zero value of σ_u would result from Eq. (11). On the contrary, even the largest bodies possess finite values of strength and toughness, as in the case of the huge floating icebergs crushing against the offshore structures (Palmer, 1991). Indeed, the fundamental scaling transition occurring in natural fractals comes into play, which has not been taken into account in the previous procedure.

4 Multifractal Scaling Laws (MFSL) for strength and toughness of heterogeneous materials

The monofractal scaling of \mathcal{G}_F and σ_u is valid only within a narrow size range, where the fractal dimension can be considered as a constant. The topological multifractality implies the progressive vanishing of fractality ($d_{\mathcal{G}} \rightarrow 0$, $d_{\sigma} \rightarrow 0$) as the scale increases. Since the microstructure of a disordered material is the same independently of the macroscopic size, the influence of disorder on the mechanical properties essentially depends on the ratio between a *characteristic internal length* l_{ch} and the external size b of the specimen. Therefore, *the effect of microstructural disorder on the mechanical behavior of materials becomes progressively less important at the largest scales, whereas it represents a fundamental feature at the smallest scales*. In particular, at the smallest scales, a Brownian disorder is the highest possible disorder, yielding, respectively for invasive and lacunar topologies, fractional scaling exponents equal to $+1/2$ and $-1/2$.

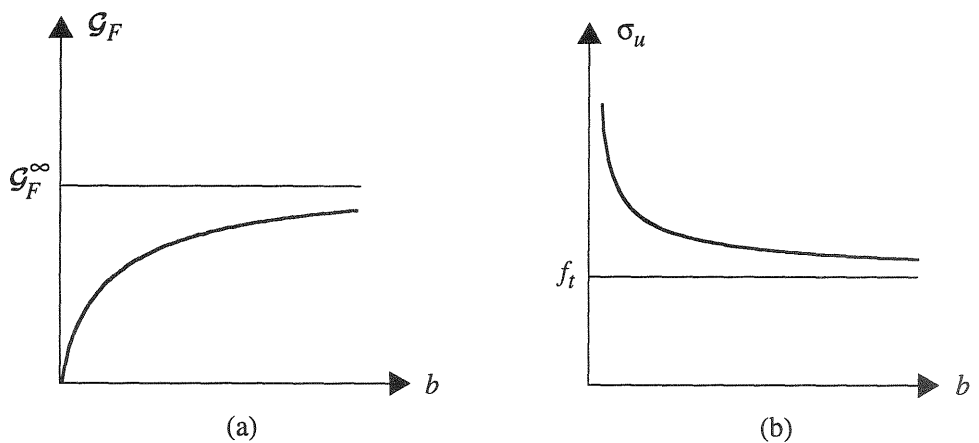


Fig. 5. Multifractal Scaling Laws for the critical parameters \mathcal{G}_F and σ_u .

On the basis of these hypotheses, two Multifractal Scaling Laws are proposed, respectively for fracture energy (Carpinteri & Chiaia, 1995b) and tensile strength (Carpinteri et al., 1995b), which can be written in the following analytical form:

$$\mathcal{G}_F(b) = \mathcal{G}_F^\infty \left[1 + \frac{l_{ch}}{b} \right]^{-1/2}, \quad (12-a)$$

$$\sigma_u(b) = f_t \left[1 + \frac{l_{ch}}{b} \right]^{1/2}. \quad (12-b)$$

These scaling laws, shown in Fig. 5, are both two-parameter models, where the asymptotic value of the nominal quantity (\mathcal{G}_F^∞ or f_t), corresponding respectively to the highest nominal fracture energy and to the lowest nominal tensile strength, is reached only in the limit of infinite sizes.

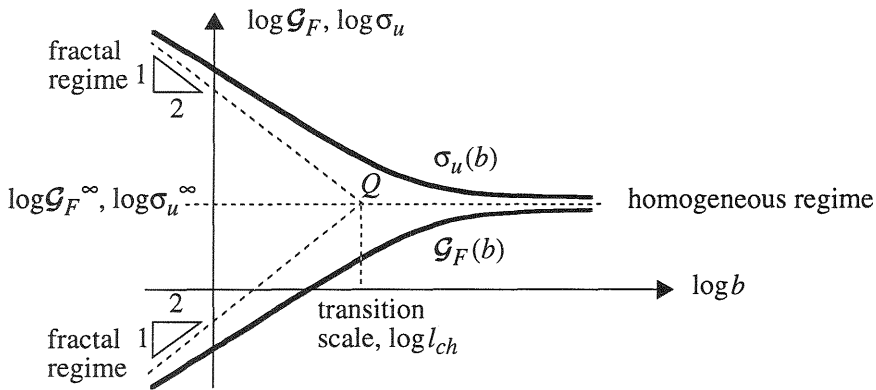


Fig. 6. Multifractal Scaling Laws: bilogarithmic diagrams.

The dimensionless term into square brackets, which is controlled by the characteristic value of the internal length l_{ch} , represents the variable influence of disorder on the mechanical behavior, thus quantifying the difference between the nominal quantity measured at the scale b and the asymptotic constant value. Note the perfect *duality* between the scaling laws, the only difference being the sign of the Brownian exponent ($\pm 1/2$), respectively related to an invasive or to a lacunar topology.

In the bilogarithmic diagrams, shown in Fig. 6, the transition from the fractal regime to the euclidean one becomes evident. The threshold of this transition is meaningfully represented by point Q , whose abscissa is equal to $\log l_{ch}$. The oblique asymptote is controlled in both cases by a quantity with the dimensions of a stress-intensity factor ($[F][L]^{-3/2}$), signifying that

LEFM comes into play only when the characteristic size a of microdefects is comparable with the external size (highest disorder), whereas, at larger scales, the correlation among the microcracks increases, leading to the homogeneization in the limit of infinite size (ordered regime).

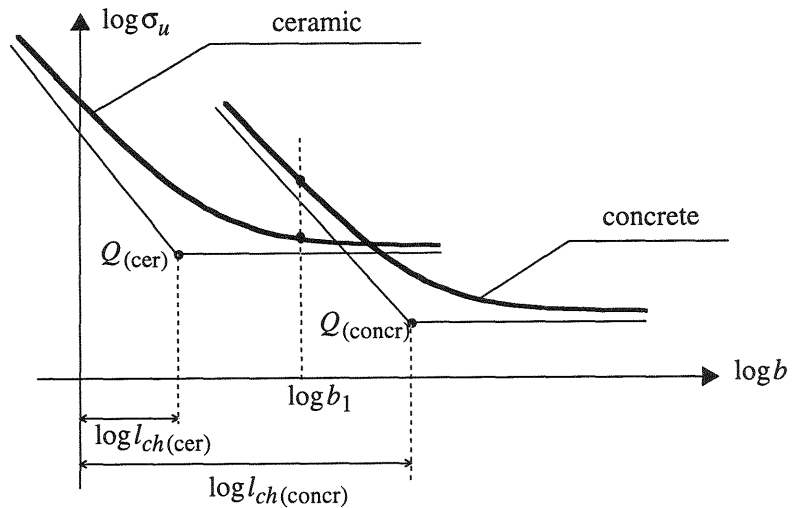


Fig. 7. Multifractal scaling of tensile strength in two different materials.

Carpinteri et al. (1995b) proposed to relate the value of the internal length l_{ch} to some characteristic size of the microstructure, for example, in the case of concrete, to the maximum aggregate size d_{max} :

$$l_{ch} = \alpha d_{max}. \quad (13)$$

This internal length parameter becomes essential when the scaling behavior of two different materials is compared, as it is shown in Fig. 7 for the scaling of tensile strength. It can be stated that, in the case of a finer grained material like a ceramic composite, the MFSL is shifted to the left with respect to the case of concrete, the value of l_{ch} being much lower for ceramics than for concrete. Therefore, two specimens of different materials, with the same structural dimension b_1 , besides obviously showing two different values of the nominal tensile strength, have to be set in two different scaling regimes. With reference to Fig. 7, the concrete specimen behaves accordingly to the fractal regime, whereas the ceramic one lies on the asymptotic branch of the MFSL, thus showing an homogeneous macroscopic behavior. Generally speaking, one has to determine for each material the proper range of scales where the fractal regime is predominant, and consequently the minimum structural size beyond which the local toughness and strength fluctuations are

macroscopically averaged and constant values of the mechanical properties can be determined.

5 Application of the MFSL to experimental tensile strength data

The Multifractal Scaling Laws described in the previous section are now applied to relevant experimental data reported in the literature. This statistical analysis aims firstly to the validation of the multifractal model by means of the *goodness of fit* of the experimental data and, subsequently, to the extrapolation of reliable values of the mechanical properties, valid for real-sized structures, starting from laboratory-sized specimens. The non-linear Levenberg-Marquardt best-fitting algorithm has been extensively used in this analysis: a complete review of all the examined references is in (Carpinteri et al., 1995b), where the Multifractal Scaling Law for tensile strength is also compared with the Bazant's Size Effect Law (Bazant, 1984). In any case, fitting of the data appears to be consistent only if (at least) one order of magnitude is considered in the size range.

Among the several three-point bending tests reported in the literature, the results are presented of the tests by Gettu et al. (1990), performed on notched *high strength concrete* beams, with average compressive strength equal to 96 MPa. This kind of material, where silica fume and fly ash are also present, is characterized by relatively small aggregates and by a strong bond between matrix and aggregates. The strength of the cementitious matrix is comparable with that of the aggregates, thus resulting in a *more homogeneous* fracture process with respect to ordinary concrete: the width of the fracture process zone, according to the cohesive model, decreases almost by 60%. Consequently, whilst the compressive strength increases almost by 160%, the material's fracture energy increases only by the 25%, the *Brittleness Number* resulting thus halved. This results in a definitely more brittle behavior with respect to ordinary concrete implying, in the Multifractal Scaling Law, the rapid transition towards the ordered regime, characterized by the absence (or, better, by the homogeneization) of the benefic contribute by microstructural disorder.

Four similar prismatic specimens have been tested, all notched at midspan and subjected to bending: the reference structural size b is chosen equal to the total beam depth (considering also the notch), that is, to 38.1, 76.2, 152.4 e 304.8 mm, respectively (range 1:8). The notch depth a_0 , scaled in a proportional manner with b , is set equal to $b/3$, whilst the net span between the supports results $L = 2.5 b$. Note that only a two-dimensional similitude is provided, the thickness t of all the specimens being constantly equal to 38.1 mm. The maximum aggregate size is

9.5 mm. The nominal tensile strength is computed according to the Theory of Elasticity, assuming as resisting section the initially uncracked ligament:

$$\sigma_u(b) = \frac{6M_u}{t(b-a_0)^2}, \quad (14)$$

where M_u is the ultimate bending moment at midspan. Fitting by the MFSL is directly plotted in the bilogarithmic diagram (Fig. 8), where the fitting by Bazant's Size Effect Law (SEL) is also shown for comparison. The computed best-fit values are: $f_t=4.1$ MPa and $l_{ch}=156.9$ mm, thus resulting in $\alpha=l_{ch}/d_{max}=16.51$. The MFSL correlation coefficient is $R=0.981$, whereas the application of SEL yields $R=0.914$. Gettu et al. believe that the strength values obtained from the largest specimens are too large, these being in clear disagreement with the SEL predictions. On the contrary, these values show perfect agreement with the MFSL, as they are placed in the asymptotic homogeneous regime of the scaling, which, in the case of high strength concrete, comes into play much earlier.

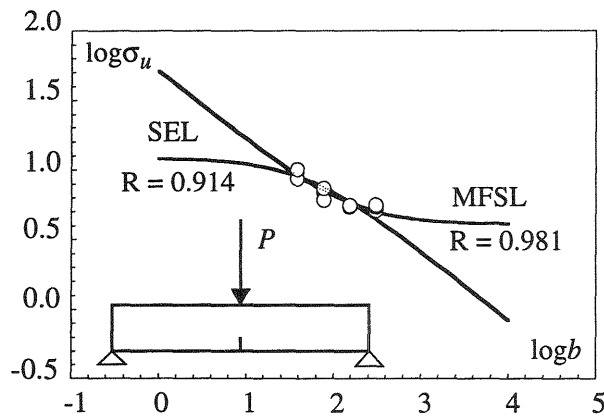


Fig. 8. Application of the MFSL to the data by Gettu et al. (1990).

Note also that the asymptotic strength f_t is equal to the 60% of the specimens' average strength ($\bar{\sigma}_m = 6.8$ MPa), and only to the 43% of the smallest specimens' one!

Another interesting test geometry is represented by the *splitting cylinder tests* carried out by Hasegawa et al. (1985). Concrete cylinders, geometrically similar in two dimensions (the height of the cylinders being constant and equal to 500 mm), have been tested in the (wide) size range 1:30 ($b_{min} = 100$ mm, $b_{max} = 3000$ mm). The maximum aggregate size is equal to 25 mm, whilst the average compressive strength results 23.4 MPa. The nominal tensile strength is supposed to be equal to the maximum

principal stress, according to the Theory of Elasticity:

$$\sigma_u(b) = \frac{2P_u}{\pi b h}, \quad (15)$$

where P_u is the ultimate load, and b and h are respectively the diameter and the (constant) height of the specimens.

The application of the MFSL is plotted directly in the bilogarithmic diagram (Fig. 9), where the fitting by Bazant's Size Effect Law (SEL) is also shown for comparison. The computed best-fitting values are: $f_t = 1.45\text{MPa}$ and $l_{ch} = 199.2\text{mm}$. Note that the asymptotic strength f_t is equal to 80% of the average ultimate tensile stresses (1.80MPa) and only to 56% of the smallest specimens' strength. On the basis of Eq. (13), the dimensionless parameter α results equal to 7.96. The correlation coefficient yielded by the MFSL is $R = 0.966$, whereas Bazant's SEL yields $R = 0.663$. Note that, in the case of tests characterized by wide size ranges, the MFSL modelizes much better than SEL the scaling behavior of tensile strength, the concavity of data being clearly upwards according to the aforementioned multifractal transition

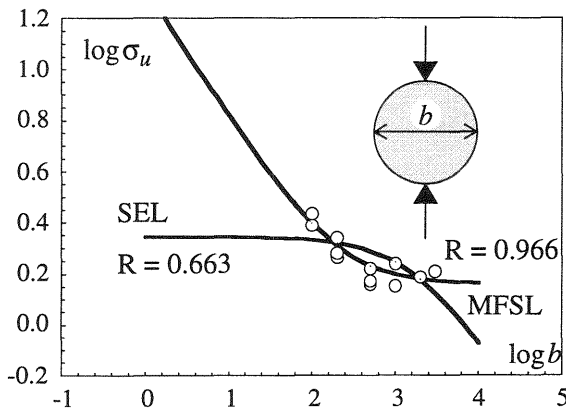


Fig. 9. Application of the MFSL to the data by Hasegawa et al. (1985).

Pull-out tests have been performed by Eligehausen et al. (1992) and by Bazant & Sener (1988). The first series consists in the extraction of anchor steel bolts from prismatic similar concrete specimens, with the dimensional ratio 1:3:9 (b =bar embedment depth= 50, 150 and 450 mm). A three-dimensional similitude is ensured by proper scaling of all the sizes of the specimens. All the specimens have been cast from the same batch of concrete, characterized by an average compressive strength equal to 30MPa and by the maximum aggregate size equal to 22mm. In all the specimens a tensile failure mechanism has been detected, consisting in the

removal of a concrete cone with height equal to the depth of the steel bar. The nominal stress at failure, computed from the ultimate load P_u , is defined according to:

$$\sigma_u(b) = \frac{P_u}{A_{cone}} = \frac{P_u}{(\pi 3b^2)/4}. \quad (16)$$

In Fig. 10a the application of MFSL and SEL to the experimental data is shown: note that the strength values have been normalized to the average compressive strength. The best-fitting values result $f_t=0.518$ MPa and $l_{ch}=438.6$ mm, yielding $\alpha=l_{ch}/d_{max}=19.9$. Fitting by the MFSL gives $R=0.996$, whereas fitting by the SEL gives $R=0.977$.

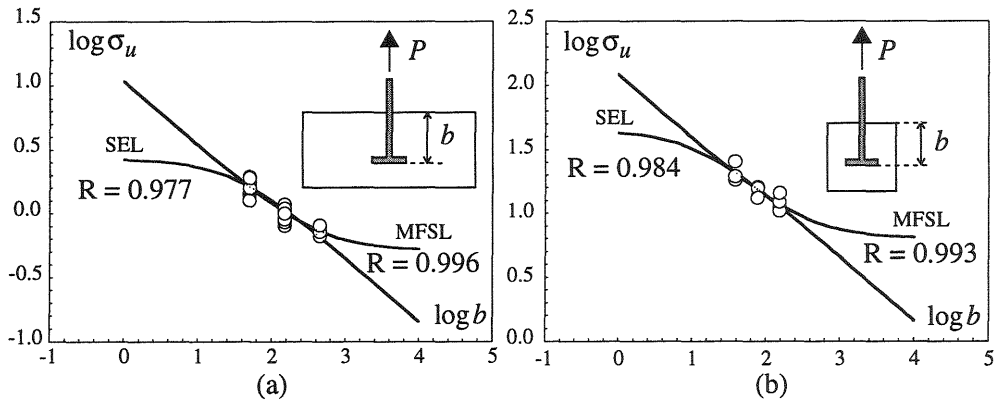


Fig. 10. Application of the MFSL: (a) to the data by Eligehausen et al. (1992) and (b) to the data by Bazant & Sener (1988).

The pull-out tests by Bazant & Sener (1988) confirm the slight upward concavity in the bilogarithmic diagram. Anyway, in this case, the size range (1:4) is too small to ensure sufficient statistical reliability. Cubic micro-concrete ($d_{max}=6.4$ mm) specimens have been tested, with average compressive strength equal to 45.8 MPa. A three-dimensional similarity is considered. The collapse mechanism results totally different from the cone failure detected by Eligehausen et al., the contrast plates acting close to the steel bar. Failure has occurred either by slipping of the bar or by splitting of the surrounding concrete, caused by the strong radial tractions originating from the bar. A conventional strength is defined according to:

$$\sigma_u(b) = \frac{P_u}{A_{adherence}} = \frac{P_u}{(\pi d_{bar}) b}, \quad (17)$$

d_{bar} and b being the diameter and the embedment depth of the bar.

The application of MFSL and SEL to the experimental data is shown in Fig. 10b. In this case the values have not been normalized. The best-fitting procedure yields $f_t=6.4$ MPa, $l_{ch}=362.5$ mm and $\alpha=l_{ch}/d_{max}=56.6$. Fitting by the MFSL gives $R=0.993$, whereas fitting by the SEL gives $R=0.984$. Note that, in this case, *the linear (monofractal) approximation of the scaling law is satisfactorily reliable, due to the narrow range of sizes that has been considered.*

6 Application of the MFSL to experimental fracture energy data

Wittmann et al. (1990) have performed a series of *compact tests* over a size range 1:4 ($b_{min}=150$ mm, $b_{max}=600$ mm, where b is the initial ligament length). The average compressive strength f_c results 42.9MPa, and the maximum aggregate size d_{max} 16 mm. A two-dimensional similitude is present, the thickness t of the specimens being constantly equal to 120mm. Six specimens have been tested for each representative size. The nominal values of the fracture energy are obtained by the ratio between the total work of fracture (area under the load-displacement curve) and the initial area of the ligament ($b \times t$). Note that the authors cut the end of the softening tail, intending that the *hinge-mechanism* due to bridging and interlocking between aggregates has not to be taken into account in the toughness evaluation.

Fitting of the \mathcal{G}_F values by means of the MFSL is shown in Fig. 11a. The asymptotic fracture energy results $\mathcal{G}_F^\infty=196.2$ N/m, and the internal length $l_{ch}=209.5$ mm. Therefore, the asymptotic toughness is about the 40% larger than the smallest specimens' value (121.5 N/m). The non-dimensional parameter α results equal to 13.1 whilst the correlation coefficient turns out to be $R=0.937$.

Experimental results obtained by rigorously following the RILEM Recommendation are those by Elices et al. (1992). Three-point bending tests under crack opening control have been carried out by the authors on beams made of concrete with $d_{max}=10$ mm and $f_c=33.1$ MPa. As in the previous case, only a two-dimensional similitude is provided, the thickness t being equal to 100mm for all the beams. The beam height, assumed as the reference size, ranges from 50mm to 300mm (range 1:6). The nominal fracture energy is obtained from the total work of fracture (considering also the weight of the beam and of the testing equipment), divided by the initial ligament ($(b-a_0) \times t$, where $a_0=b/3$ is the initial notch depth). The application of the MFSL is shown in Fig. 11b: the best-fitting values are respectively $\mathcal{G}_F^\infty=110.6$ N/m and $l_{ch}=133.1$ mm. The asymptotic fracture energy results the 90% larger than the smallest specimens' value (57N/m).

The non-dimensional parameter $\alpha = l_{ch} / d_{max}$ is equal to 13.3, and the correlation coefficient turns out to be $R=0.982$.

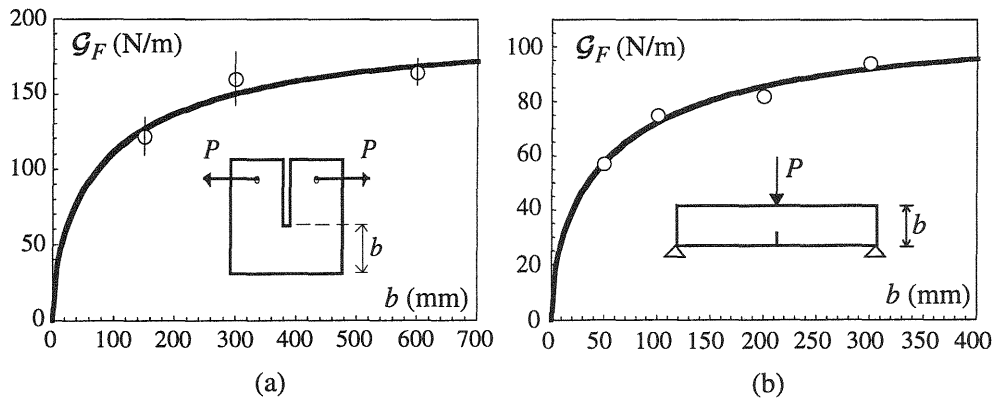


Fig. 11. Application of the MFSL: (a) to the data by Wittmann et al. (1990) and (b) to the data by Elices et al. (1992).

Kim et al. (1992) have performed wedge-splitting tests on concrete with different compressive strengths and maximum aggregate size equal to 7 mm, detecting a strong dependence of the nominal fracture energy on the specimen size (range=1:5). The nominal fracture energy is obtained as the total work of fracture (computed from the load-displacement diagram) divided by the initial ligament. In Fig. 12a the application of the MFSL to the experimental data is shown: in the case of the 20 MPa concrete, non linear fitting yields the asymptotic fracture energy $\mathcal{G}_F^\infty = 88.3 \text{ N/m}$, and the characteristic internal length $l_{ch} = 86.1 \text{ mm}$, whereas, in the case of the 100 MPa concrete, the following parameters are determined: $\mathcal{G}_F^\infty = 102.1 \text{ N/m}$ and $l_{ch} = 38.9 \text{ mm}$. Note that, even if the asymptotic fracture energy, in the case of the stronger mixture, is larger than in the case of the 20 MPa concrete, the internal length results smaller, thus indicating the more rapid homogenization (vanishing of fractality) occurring in the scaling behavior of the stronger concrete.

Zhong (1991) performed wedge-splitting tests on two series of concrete with different maximum grain size, 8 mm and 32 mm respectively. The examined size range is equal to 1:8 in the case of the finer mixture and to 1:20 in the case of the coarse one. In Fig. 12b the application of the MFSL to the experimental data is shown: in the case of the finer grained concrete, non linear fitting yields the asymptotic fracture energy $\mathcal{G}_F^\infty = 78.9 \text{ N/m}$, and the characteristic internal length $l_{ch} = 5.6 \text{ mm}$ ($\alpha = 0.7$), whereas, in the case of the coarse grained concrete, the following parameters are determined: $\mathcal{G}_F^\infty = 89.1 \text{ N/m}$ and $l_{ch} = 11.8 \text{ mm}$ ($\alpha = 0.37$).

The correlation coefficient R results equal to 0.997 and to 0.881, for the finer and the coarser mix respectively. As expected, concrete with a larger maximum aggregate size has a higher asymptotic fracture energy.

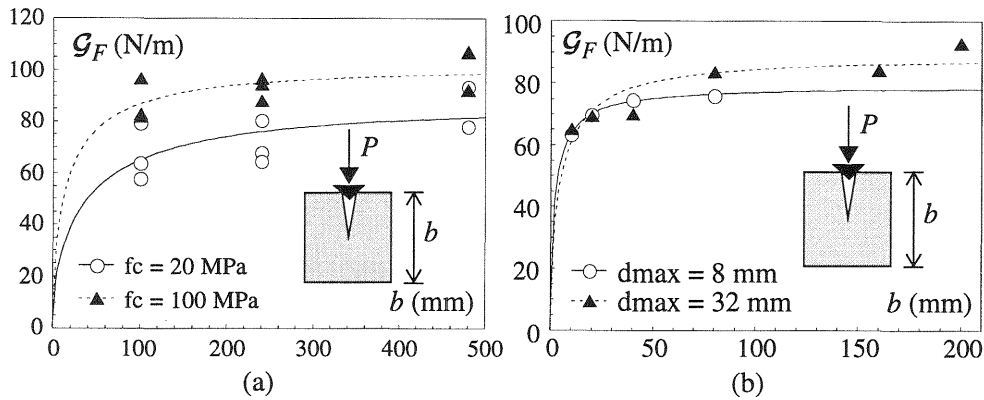


Fig. 12. Application of the MFSL: (a) to the data by Kim et al. (1992) and (b) to the data by Zhong (1991).

Moreover, it is interesting to point out that the coarse mixture yields a larger internal length, according to the MFSL, and therefore the transition to the homogeneous behavior occurs later than in the case of the 8 mm mixture. It is therefore confirmed that the value of l_{ch} is intimately related to the maximum aggregate size, as already proposed by the authors.

7 References

- Barenblatt, G.I. & Botvina, L.R. (1983). Self-similarity of fatigue fracture. Defect accumulation. *Izv. AN. SSSR. Mech. Tv. Tela*, 4, 161-165.
- Barenblatt, G.I. (1993). Intermediate asymptotics, scaling laws and renormalization group in continuum mechanics. *Meccanica*, 28, 177-184.
- Bazant, Z.P. (1984). Size effect in blunt fracture: concrete, rock, metal. *Journal of Engineering Mechanics, ASCE*, 110, 518-535.
- Bazant, Z.P. & Sener, S. (1988). Size effect in pullout tests. *ACI Materials Journal*, 85, 347-351.
- Carpinteri, A. (1986). *Mechanical Damage and Crack Growth in Concrete: Plastic Collapse to Brittle Fracture*. Martinus Nijhoff Publishers, Dordrecht.

- Carpinteri, A. (1994a). Fractal nature of material microstructure and size effects on apparent mechanical properties. **Mechanics of Materials**, 18, 89-101.
- Carpinteri, A. (1994b). Scaling laws and renormalization groups for strength and toughness of disordered materials. **International Journal of Solids and Structures**, 31, 291-302.
- Carpinteri, A. (1995). Strength and toughness in disordered materials (complete and incomplete similarity). **Proceedings of the IUTAM Symposium on Size-Scale Effects in the Failure Mechanisms of Materials and Structures**, (Carpinteri, A. ed.), Torino.
- Carpinteri, A. & Chiaia, B. (1995a). Multifractal nature of concrete fracture surfaces and size effects on nominal fracture energy. In press on **Materials and Structures**.
- Carpinteri, A. & Chiaia, B. (1995b). Multifractal scaling law for the fracture energy variation of concrete structures. **Proceedings of the Second International Conference on Fracture Mechanics of Concrete Structures, FRAMCOS2**, (Wittmann, F.H. ed.), Zürich.
- Carpinteri, A., Chiaia, B. and Maradei, F. (1995a). Experimental determination of the fractal dimension of disordered fracture surfaces. **Advanced Technology on Design and Fabrication of Composite Materials and Structures**, (Carpinteri, A. & Sih, G. eds.), Kluwer Academic Publishers, Dordrecht.
- Carpinteri, A., Chiaia, B. and Ferro, G. (1995b). Multifractal scaling law: an extensive application to nominal strength size effect of concrete structures. **Internal Report of the Department of Structural Engineering**, Politecnico di Torino, Torino.
- Elices, M., Guinea, G.V. and Planas, J. (1992). Measurement of the fracture energy using three-point bend tests: Part 3 – Influence of cutting the $P-\delta$ tail. **Materials and Structures**, 25, 327-334.
- Eligehausen, R., Bouska, P., Cervenka, V. and Pukl, R. (1992). Size effect of the concrete cone failure load of anchor bolts. **Proceedings of the First International Conference on Fracture Mechanics of Concrete Structures, FRAMCOS1**, (Bazant ed.), Breckenridge, 517-525.
- Gettu, R., Bazant, Z.P. and Karr, M.E. (1990). Fracture properties and brittleness of high-strength concrete. **ACI Materials Journal**, 87, 608-618.
- Hasegawa, T., Shioya, T. and Okada, T. (1985). Size effect on splitting tensile strength of concrete. **Proceedings of the 7th Conference of the Japan Concrete Institute, JCI**, 309-312.

- Herrmann, H.J. and Roux, S. (Eds.) (1990) **Statistical Models for the Fracture of Disordered Media**. North Holland, Amsterdam.
- Kim, J.K., Mihashi, H., Kirikoshi, K. and Narita, T. (1992). Fracture energy of concrete with different specimen sizes and strength by wedge splitting test. **Proc. of the First International Conference on Fracture Mechanics of Concrete Structures, FRAMCOS1**, (Bazant Z.P. ed.), Breckenridge, 561-566.
- Mandelbrot, B.B., Passoja, D.E. and Paullay, A.J. (1984). Fractal character of fracture surfaces of metals. **Nature**, 308, 721-722.
- Palmer, A.C. and Sanderson, T.J.O. (1991). Fractal crushing of ice and brittle solids. **Proc. of the Royal Society of London**, A 433, 469-477.
- RILEM Technical Committee 50 (1985). Determination of the fracture energy of mortar and concrete by means of three-point bend tests on notched beams. Draft Recommendation. **Materials and Structures**, 18, 287-290.
- Wilson, K.G. (1971). Renormalization group and critical phenomena. **Physical Review**, B4, 3174-3205.
- Wittmann, F.H., Mihashi, H. and Nomura, N. (1990). Size effect on fracture energy of concrete. **Engineering Fracture Mechanics**, 35, 107-115.
- Zhong, H. (1991). Some experiments to study the influence of size and strength on fracture energy. **Internal Report of the Institute for Building Materials**, Swiss Federal Institute of Technology, Zürich.